

# UC San Diego

## UC San Diego Previously Published Works

### Title

Comparison of Binding Characteristics and In Vitro Activities of Three Inhibitors of Vascular Endothelial Growth Factor A

### Permalink

<https://escholarship.org/uc/item/3408m1cv>

### Journal

Molecular Pharmaceutics, 11(10)

### ISSN

1543-8384

### Authors

Yang, Jihong  
Wang, Xiangdan  
Fuh, Germaine  
[et al.](#)

### Publication Date

2014-10-06

### DOI

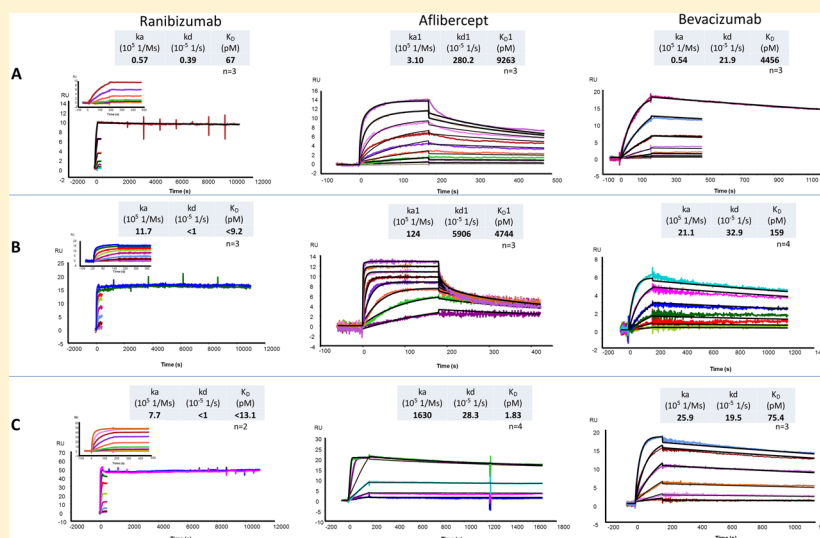
10.1021/mp500160v

Peer reviewed

# Comparison of Binding Characteristics and In Vitro Activities of Three Inhibitors of Vascular Endothelial Growth Factor A

Jihong Yang, Xiangdan Wang, Germaine Fuh, Lanlan Yu, Eric Wakshull, Mehraban Khosraviani, Eric S. Day, Barthélemy Demeule, Jun Liu, Steven J. Shire, Napoleone Ferrara,<sup>†</sup> and Sandeep Yadav\*<sup>‡</sup>

Genentech, Inc., 1 DNA Way, MS 56-2A, South San Francisco, California 94080, United States



**ABSTRACT:** The objectives of this study were to evaluate the relative binding and potencies of three inhibitors of vascular endothelial growth factor A (VEGF), used to treat neovascular age-related macular degeneration, and assess their relevance in the context of clinical outcome. Ranibizumab is a 48 kDa antigen binding fragment, which lacks a fragment crystallizable (Fc) region and is rapidly cleared from systemic circulation. Aflibercept, a 110 kDa fusion protein, and bevacizumab, a 150 kDa monoclonal antibody, each contain an Fc region. Binding affinities were determined using Biacore analysis. Competitive binding by sedimentation velocity analytical ultracentrifugation (SV-AUC) was used to support the binding affinities determined by Biacore of ranibizumab and aflibercept to VEGF. A bovine retinal microvascular endothelial cell (BREC) proliferation assay was used to measure potency. Biacore measurements were format dependent, especially for aflibercept, suggesting that biologically relevant, true affinities of recombinant VEGF (rhVEGF) and its inhibitors are yet to be determined. Despite this assay format dependency, ranibizumab appeared to be a very tight VEGF binder in all three formats. The results are also very comparable to those reported previously.<sup>1–3</sup> At equivalent molar ratios, ranibizumab was able to displace aflibercept from preformed aflibercept/VEGF complexes in solution as assessed by SV-AUC, whereas aflibercept was not able to significantly displace ranibizumab from preformed ranibizumab/VEGF complexes. Ranibizumab, aflibercept, and bevacizumab showed dose-dependent inhibition of BREC proliferation induced by 6 ng/mL VEGF, with average IC<sub>50</sub> values of 0.088 ± 0.032, 0.090 ± 0.009, and 0.500 ± 0.091 nM, respectively. Similar results were obtained with 3 ng/mL VEGF. In summary Biacore studies and SV-AUC solution studies show that aflibercept does not bind with higher affinity than ranibizumab to VEGF as recently reported,<sup>4</sup> and both inhibitors appeared to be equipotent with respect to their ability to inhibit VEGF function.

**KEYWORDS:** ranibizumab, aflibercept, bevacizumab, VEGF, affinity, analytical ultracentrifugation

## INTRODUCTION

The determination of binding affinity of a therapeutic protein to a target is an integral part of pharmaceutical development. A widely used methodology for assessing tight interactions is based on surface plasmon resonance (SPR) such as Biacore.<sup>5</sup> One caveat in this technology is that it requires ligand immobilization to a surface and it has been shown that orientation, method of binding, and which ligand is bound are

important variables that govern the determination of affinity constants.<sup>6,7</sup>

**Received:** February 25, 2014

**Revised:** August 22, 2014

**Accepted:** August 27, 2014

**Published:** August 27, 2014

Alternatively, analytical ultracentrifugation (AUC) can be used as an orthogonal free-solution technique that circumvents the potential artifacts of matrix/stationary phase or chemical modifications associated with SPR. AUC has been widely used in the biophysical characterization of proteins to determine weight-average molecular mass, sedimentation coefficient, frictional coefficient associated with molecular shape, bimolecular interactions involving reversible associations or complex formation, self-association of glycosylated and nonglycosylated proteins, and competitive binding of anti-IgE antibodies to IgE and also as an orthogonal technique to size exclusion chromatography to determine the presence of aggregates.<sup>8</sup> In addition to being able to detect the presence of protein aggregates, AUC analysis allows measurements directly in the formulation buffer or condition of interest, thereby avoiding common size exclusion HPLC limitations of protein-resin interactions and significant dilution in the elution buffer that can potentially alter the size distribution of the self-associates and aggregates, as highlighted in the above studies. One aspect of this work is to assess AUC as an orthogonal technique to SPR in evaluating the binding of therapeutic proteins, highlighting that caution must be exercised while relying on SPR results. In addition, the recent development of fluorescence optics in the analytical ultracentrifuge<sup>9,10</sup> combined with the use of fluorescently labeled material can provide definitive information about the type of complex formed.

There have been several SPR studies and potency assessments of inhibitors of vascular endothelial growth factor A (VEGF),<sup>2–4,11,12</sup> a key driver of the vascular leakage and neovascularization seen in intraocular vascular diseases including age-related macular degeneration (wet AMD), retinal vein occlusion (RVO), and diabetic macular edema (DME).<sup>1</sup> VEGF inhibitors such as ranibizumab, aflibercept, and bevacizumab are used intravitreally in patients with wet AMD, RVO, and DME. The US Food and Drug Administration has approved ranibizumab for the treatment of wet AMD, RVO, and DME<sup>13</sup> and aflibercept for the treatment of wet AMD and central RVO.<sup>14</sup> Bevacizumab is used off-label. A recent SPR study concludes that aflibercept binds to VEGF with much higher affinity than ranibizumab.<sup>4</sup> Herein we report the results of the determination of affinity constants for binding of VEGF to ranibizumab, aflibercept, and bevacizumab by SPR using different assay formats as well as the potency of inhibition of VEGF. In addition, a novel solution based competitive analytical ultracentrifuge method is used to support our conclusions.

## MATERIALS AND METHODS

Lucentis (ranibizumab) and Avastin (bevacizumab) were obtained from Genentech, Inc., South San Francisco, CA. Eylea (aflibercept; Regeneron, Inc., Tarrytown, NY) was obtained commercially. Recombinant human VEGF<sub>165</sub> (rhVEGF) was expressed and purified at Genentech. Anti-Fab antibody was obtained from GE Healthcare (Pittsburgh, PA), and protein A was obtained from Thermo Fisher Scientific, Pierce Protein Biology Products (Rockford, IL).

**SPR Binding Assays.** Binding kinetics and affinities of inhibitors of rhVEGF were assessed using surface plasmon resonance technology on a Biacore T200 instrument (GE Healthcare, Pittsburgh, PA). A series of analyte concentrations were prepared in HBS-EP running buffer (0.01 M HEPES, 0.15 M NaCl, 3 mM EDTA, and 0.05% surfactant Polysorbate 20) and injected at a flow rate of 50  $\mu$ L/min for 3 min over flow

cells (FCs) of Series S CMS sensor chips immobilized with ligand molecules at various densities depending on assay formats.

In format 1, rhVEGF was the ligand immobilized directly onto FCs at  $\sim$ 20 resonance units (RU) density, while the inhibitors were the analytes. The dissociation of inhibitors from the immobilized rhVEGF was allowed to proceed for 5 min for all samples except for the ranibizumab and bevacizumab samples with the highest concentration (200 nM), in which dissociation proceeded for 3 h or 15 min, respectively. All experiments were carried out at 37  $^{\circ}$ C.

In format 2, the inhibitors were the immobilized ligands and rhVEGF was the analyte in the mobile phase. The final ligand density was 22–45 RU. The dissociation of the analytes from the immobilized ligand was allowed to proceed for 5 min for all samples except for the ranibizumab sample with the highest concentration (200 nM), in which dissociation proceeded for 3 h. The dissociation time for all bevacizumab samples was 20 min. All experiments were carried out at 37  $^{\circ}$ C.

In format 3, the inhibitors were immobilized indirectly to the sensor chip using anti-human IgG Fab antibody or protein A as capturing molecules as previously reported.<sup>4</sup> Rigorous surface testing was conducted in the current study to evaluate the validity of the method for all inhibitors. The densities of the capture molecules were  $\sim$ 11000 or 1000 RU for anti-human IgG Fab antibody and  $\sim$ 5500 RU for protein A. The final ligand density used was  $\sim$ 28 RU for the indirectly captured ranibizumab,  $\sim$ 40 RU for bevacizumab, and  $\sim$ 50 RU for aflibercept. The dissociation of the analytes from the immobilized ligand was allowed to proceed for 5 min for ranibizumab samples except for the sample with the highest concentration (200 nM), in which dissociation proceeded for 3 h. The dissociation time for all aflibercept and bevacizumab samples was 30 min. Experiments were carried out at 37  $^{\circ}$ C or 25  $^{\circ}$ C for this format.

Sensorgrams of ranibizumab, aflibercept, and bevacizumab binding to rhVEGF using all three formats were analyzed to obtain kinetic data and affinities using Biacore T200 Evaluation Software (version 2.0.1; GE Healthcare). Because of the dimeric nature of rhVEGF and the presence of two potential binding sites in all inhibitors except ranibizumab, definitive monovalent binding affinities for rhVEGF and its inhibitors can be challenging to obtain. Very low immobilization densities were used to encourage monovalent binding, and the presence of such interactions were evaluated using a 1:1 Langmuir binding model. In all but two conditions tested, the 1:1 binding model was sufficient to describe interactions between rhVEGF and its inhibitors. The dissociation rate constant ( $k_d$ ) and association rate constant ( $k_a$ ) were obtained via kinetic fitting, and the equilibrium dissociation constant ( $K_D$ ) was derived by taking the ratio of  $k_d$  over  $k_a$  calculated using the simplest 1:1 binding model. Only in cases where aflibercept was evaluated in formats 1 and 2 was the 1:1 binding model insufficient to describe interactions between the inhibitor and rhVEGF. In those cases a bivalent analyte binding model was used and the first equilibrium dissociation constant ( $K_{D1}$ ), first dissociation rate constant ( $k_{d1}$ ), and first association rate constant ( $k_{a1}$ ) were reported.

**Competitive Binding Assessed by Sedimentation Velocity Analytical Ultracentrifugation (SV-AUC).** Each molecule individually and preformed complexes between ranibizumab and VEGF and aflibercept and VEGF were first evaluated to obtain their sedimentation coefficients. After this,

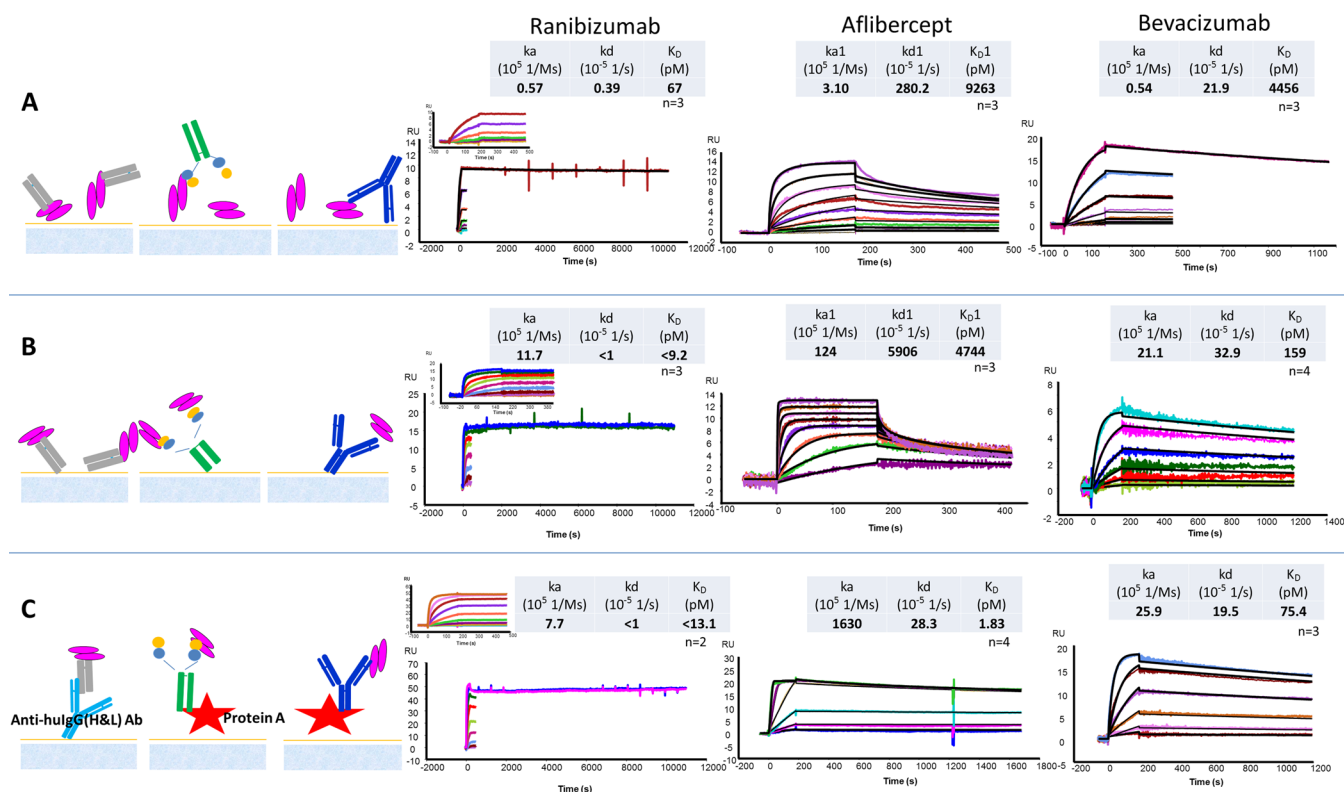


**Figure 1.** Binding of rhVEGF–anti-VEGF inhibitor molecules in Biacore assays. (A) rhVEGF is the ligand immobilized directly onto the flow cell (FC), while the inhibitors were the analytes injected over the FC at varying concentrations (format 1). (B) VEGF inhibitors immobilized as ligand with VEGF in the mobile phase as analyte (format 2). (C) Inhibitors immobilized indirectly to the sensor chip with VEGF in the mobile phase as analyte (format 3). Note: limit of  $k_d$  that can be accurately measured by the instrument is  $\sim 5 \times 10^{-6} \text{ s}^{-1}$ . To be conservative, a  $k_d < 10^{-5} \text{ s}^{-1}$  was chosen.

competition experiments were conducted using a preformed inhibitor/VEGF complex challenged with a different VEGF inhibitor to assess whether the previously reported  $\sim 100$ -fold higher affinity of aflibercept to rhVEGF compared with ranibizumab<sup>4</sup> is valid in free solution, i.e., no binding to a surface as in SPR measurements.

Experiments were performed at room temperature in PBS, pH 7.2 (137 mM NaCl, 27 mM KCl, 8 mM Na<sub>2</sub>HPO<sub>4</sub>, and 1.5 mM KH<sub>2</sub>PO<sub>4</sub>). Alexa Fluor 488 protein labeling kits were purchased from Molecular Probes (Eugene, OR). All chemicals used were reagent grade or higher. Alexa Fluor 488 labeled ranibizumab (denoted as ranibizumab\*) was produced as recommended by the manufacturer.

Sedimentation velocity experiments were performed in an Optima XL-I analytical ultracentrifuge equipped with absorbance optics, interference optics (Beckman Coulter, Fullerton, CA), and fluorescence optics (Aviv Biomedical) in centrifuge cells with 12 mm graphite-filled Epon centerpieces (Spin Analytical, Durham, NH) at 20 °C and rotor speed of 40000 rpm. Quartz windows were used when using the absorbance optics, and the scans were acquired at a wavelength of 230 nm at 30  $\mu\text{m}$  radial increments. When using the fluorescence optics, sapphire windows were used, and the data were acquired at 20  $\mu\text{m}$  radial increments averaging five revolutions per scan. The sedimentation boundaries were analyzed with SEDFIT, version 11.3 and 11.72c.<sup>15</sup> The resulting continuous,  $c(s)$ , distribution with 70% confidence level was calculated after optimizing baseline, meniscus, and cell bottom positions by nonlinear regression. All  $s$  values obtained with the  $c(s)$  distribution in

PBS were converted to  $s_{20,w}$  with SEDNTERP (version 1.09) using the measured density and viscosity of PBS.

**Bovine Retinal Microvascular Endothelial Cell (BREC) Proliferation Assay.** A BREC assay was used because bovine microvascular endothelial cells are well established as a cell type that is highly responsive to growth factors such as VEGF and bFGF.<sup>16</sup> Unlike another cell line that has been used to assess potency, HUVEC, which is derived from a large vessel, BREC is a more physiologically relevant cell type to investigate angiogenesis.

BREC proliferation assays were performed as previously described.<sup>12</sup> Cells were seeded in 96-well plates in low glucose DMEM (supplemented with 10% heat-inactivated calf serum, 2 mM glutamine, and antibiotics) at a density of 500 cells/well. Ranibizumab and aflibercept were tested from 0.004 to 10 nM, while bevacizumab was tested from 0.04 to 90 nM. Twenty minutes after addition of inhibitors, VEGF was added to a final concentration of 6 ng/mL (0.15 nM) or 3 ng/mL (0.075 nM). After 6 days, cell growth was assayed with the use of alamarBlue (BioSource). Fluorescence was measured at 530 nm excitation wavelength and 590 nm emission wavelength. IC<sub>50</sub> values were calculated using KaleidaGraph. For statistical analysis, one-way ANOVA was used, followed by the Tukey–Kramer HSD test comparing all pairs.

## RESULTS

**Binding Affinities and Kinetics of VEGF Inhibitors Using SPR Technology.** *Format 1.* rhVEGF, an antiparallel homodimer, was the immobilized ligand with inhibitors in the mobile phase as analytes (Figure 1A). Binding of ranibizumab

followed a simple monovalent (1:1) analyte binding model as expected because the Fab molecule has only one VEGF binding site. This was clearly shown by the closeness of the fit to the experimental data (Figure 1A). Aflibercept and bevacizumab each contained two VEGF-binding sites. Using very low rhVEGF immobilization levels, binding of these two inhibitors to rhVEGF was encouraged to favor monovalent binding.<sup>17,18</sup> This approach worked for bevacizumab since the 1:1 binding model sufficiently described the interactions between the inhibitor and rhVEGF (Figure 1A). However, in the case of aflibercept, even the lowest immobilization level of rhVEGF was insufficient to completely shift the interaction to monovalent binding, and attempts to fit the data with a 1:1 Langmuir binding model failed (data not shown). Therefore, a bivalent analyte binding model was used considering each aflibercept molecule has two potential VEGF binding sites. Although the curve fits still deviated from the experimentally obtained results (Figure 1A), the overall quality of the fit was much improved over that obtained from using a 1:1 binding model (data not shown). The challenge in fitting the aflibercept binding curves may be due to the global fit bivalent model that allows individual bulk effect correction to accommodate baseline drift,<sup>18</sup> although other factors such as binding induced conformational change cannot be ruled out. Because the second step in the bivalent analyte binding model involves intramolecular binding on a sensor chip without an increase in mass, only two-dimensional kinetics for the second step are obtained. The first step kinetics from a bivalent analyte binding model are most relevant in understanding the binding kinetics and strength between an analyte and a ligand. Therefore, only first kinetic parameters ( $k_{a1}$ ,  $k_{d1}$ ) and first  $K_{D1}$  were shown for aflibercept binding to rhVEGF. Although the (first) association rate constants for all three inhibitors were similar, ranibizumab had a much slower dissociation rate constant ( $0.39 \times 10^{-5} \text{ s}^{-1}$ ) than aflibercept and bevacizumab ( $280.2 \times 10^{-5}$  and  $21.9 \times 10^{-5} \text{ s}^{-1}$ , respectively). As a result, ranibizumab showed a lower  $K_D$  value (67 pM) than aflibercept (9263 pM) or bevacizumab (4456 pM) (Figure 1A, insets).

**Format 2.** The inhibitors were the immobilized ligands with rhVEGF in mobile phase as the analyte (Figure 1B). Since each rhVEGF has two potential binding sites for the immobilized inhibitor molecules, experimental conditions were again optimized to encourage monovalent interactions by using low ligand immobilization levels. Similar to format 1, the fits using the 1:1 binding model for both ranibizumab and bevacizumab showed reasonable agreement to the experimentally obtained results (Figure 1B); for aflibercept, much discrepancy was once again observed between the experimental data and the fitted curves using the 1:1 binding model (data not shown). Therefore, the bivalent analyte binding model was used, and first kinetic parameters and dissociation equilibrium constant were summarized in Figure 1B, inset. Ranibizumab again dissociated much more slowly than the other two inhibitors, and a very conservative limit ( $1 \times 10^{-5} \text{ s}^{-1}$ ) of  $k_d$  was used in order to confidently assess the upper limit of  $K_D$  value. Even with this conservative approach, ranibizumab showed a higher binding affinity than aflibercept and bevacizumab, with  $K_D$  ( $K_{D1}$ ) values of <9.2, 4744, and 159 pM, respectively (Figure 1B, insets). Comparing results obtained from format 2 and format 1 revealed some interesting observations: the (first) association rate constants  $k_a$  for all three inhibitors were higher using format 2 than format 1. While it is challenging to know exactly how different the  $k_d$  values were for ranibizumab, both

formats showed very slow dissociation. The  $k_d$  ( $k_{d1}$ ) values obtained from both formats were very similar for bevacizumab but not for aflibercept (Figure 1A,B, insets).

**Format 3.** The inhibitors were immobilized indirectly to the sensor chip using anti-human IgG Fab antibody or protein A as capturing molecules following surface testing to evaluate the validity of the method for all VEGF inhibitors (Figure 1C). While the levels of captured aflibercept and bevacizumab (not shown) stayed almost the same during the time needed for kinetic analysis (Figure 2A), a significant amount of

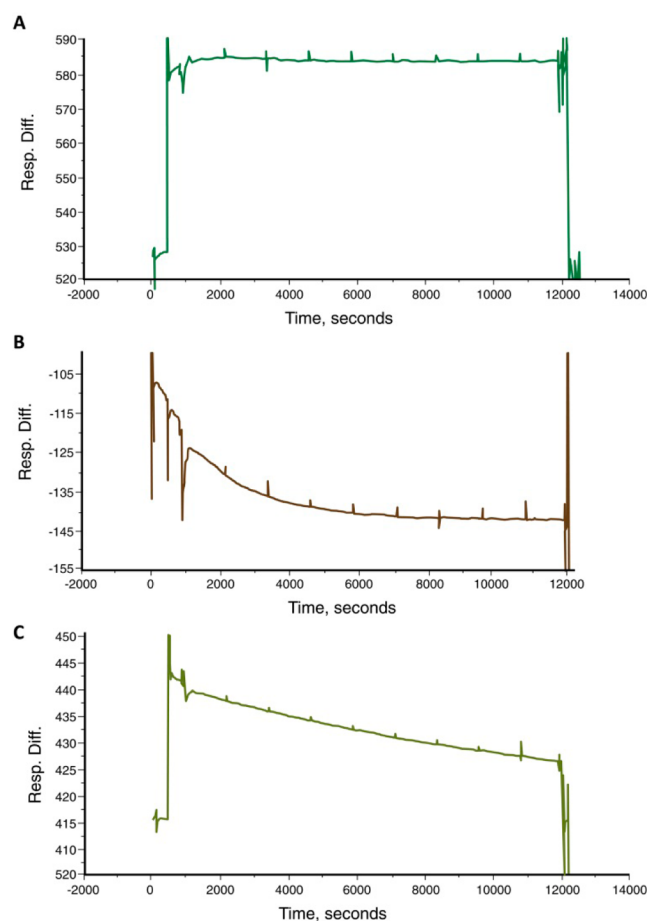


**Figure 2.** Levels of aflibercept and ranibizumab captured by an anti-Fab antibody or protein A. (A) Level of aflibercept captured by protein A over 3 h in an indirect capturing format at 37 °C. Level of protein A immobilized was approximately 5500 RU. Aflibercept was indirectly captured at approximately 50 RU. (B) Level of ranibizumab captured by anti-Fab antibody over 3 h in an indirect capturing format at 37 °C. Level of anti-Fab antibody immobilized on the sensor chip was approximately 11000 RU. Ranibizumab was indirectly captured at approximately 28 RU. (C) Level of ranibizumab captured by the anti-Fab antibody over 3 h in an indirect capturing format at 25 °C. Level of anti-Fab antibody immobilized on the sensor chip was approximately 1000 RU. Ranibizumab was indirectly captured at approximately 27 RU.

ranibizumab dissociated from the anti-Fab antibody capture molecule: signal decreased nearly 100% when anti-Fab antibody was immobilized at 11000 RU at 37 °C (Figure 2B) and more than 50% when anti-Fab antibody was immobilized at 1000 RU at 25 °C (Figure 2C), a condition reported in the literature.<sup>4</sup> These results indicated that this anti-Fab antibody is not suitable to capture ranibizumab for affinity measurements. We

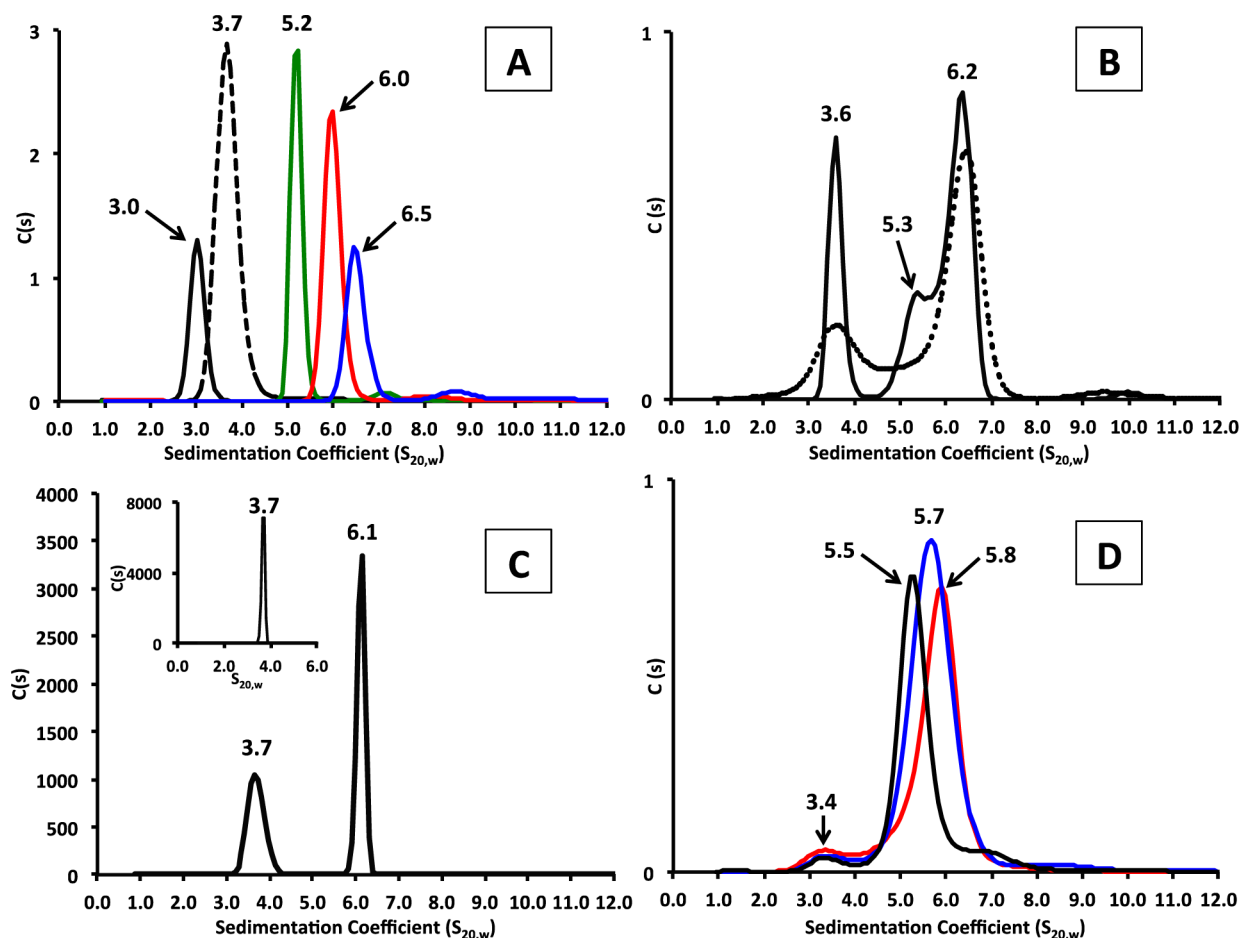


**Figure 3.** Analytical ultracentrifugation analysis. (A) Continuous sedimentation coefficient distribution of VEGF (solid black trace), ranibizumab (dashed black trace), aflibercept (green trace), 2:1 ranibizumab/VEGF complex (red trace), and 1:1 aflibercept/VEGF complex (blue trace) in PBS at a total protein concentration of 0.1 mg/mL. The 2:1 ranibizumab/VEGF complex and 1:1 aflibercept/VEGF complex were prepared on a molar basis. Ranibizumab, VEGF, and aflibercept were 99% monomeric and did not reveal the presence of aggregate missed by SE-HPLC. Aflibercept showed a small amount of higher order species around 7.1 S, which appears to be present in 1:1 aflibercept/VEGF complex, as well as at 8.7 S. The higher order species were present at a low enough concentration to be considered insignificant. (B) Competition profile of a solution containing 1 mol equiv of ranibizumab (dotted line) or 2 mol equiv of ranibizumab (solid line) added to preformed 1:1 aflibercept/VEGF complex. The addition of ranibizumab to the aflibercept/VEGF complex displaced aflibercept, which appears as a monomer at 5.3 S. (C) The continuous sedimentation coefficient distribution for labeled ranibizumab\* (inset) and 2 mol equiv of ranibizumab\* (labeled) added to preformed 1:1 aflibercept/VEGF complex in PBS measured using the fluorescence detection system (FDS) optics. The total concentration of labeled ranibizumab\* was maintained at 200 nM. The preformed 1:1 aflibercept/VEGF complex in PBS was challenged with 2 mol equiv of labeled ranibizumab\*. The sedimentation coefficient distribution clearly shows the formation of a ranibizumab/VEGF complex. (D) The sedimentation profile of various complexes where a preformed 2:1 ranibizumab/VEGF complex was titrated with different amounts of aflibercept in PBS. The total protein concentration was maintained at 0.1 mg/mL. A preformed 2:1 ranibizumab/VEGF complex was challenged with 0.5 mol equiv (red trace), 1 mol equiv (blue trace), and 4 mol equiv (black trace) of aflibercept. Aflibercept was not able to materially displace ranibizumab from the ranibizumab/VEGF complex.

were able to obtain a stable level of captured ranibizumab by using an antibody specific to huIgG heavy and light chain (Jackson ImmunoResearch Laboratories, Inc., West Grove, PA). The results for ranibizumab were similar to those obtained in format 2, with an equilibrium dissociation constant of less than 13.1 pM using a conservative estimation of the  $k_d$  value (Figure 1C, inset). In contrast, the results for aflibercept in this assay format were drastically different from the ones obtained in the first two assay formats: first of all, a simple 1:1 binding model was sufficient to describe the interactions between aflibercept and rhVEGF using format 3; in addition, the  $k_a$  value was over 500- and 10-fold higher than  $k_{a1}$ 's obtained from formats 1 and 2, respectively; conversely, the  $k_d$  value was about 10- and 200-fold smaller than the  $k_{d1}$ 's derived from formats 1 and 2, respectively. These kinetic differences resulted in  $K_D$

( $K_{D1}$ ) values for aflibercept ranging from 1.83 to 9263 pM (Figure 1, insets). The  $K_D$  of 1.83 pM for aflibercept is similar to what was reported by Papadopoulos et al.,<sup>4</sup> although the experiment reported here was conducted at 37 °C rather than 25 °C. The association rate constant for aflibercept as determined in this format,  $1.63 \times 10^8 \text{ M}^{-1} \text{ s}^{-1}$ , is extremely fast and may have exceeded the instrument's limit for reliable measurement. The results for bevacizumab were similar to the ones in format 2 with similar  $k_a$ ,  $k_d$ , and  $K_D$  values, obtained using a 1:1 binding model (Figures 1B,C, insets). The  $K_D$  for bevacizumab was 75.4 pM as determined using format 3. Comparing kinetics obtained from format 3, it is interesting to note that both ranibizumab and aflibercept have very high affinities in their binding to VEGF, although the main drivers

for those tight interactions are quite different since ranibizumab dissociated very slowly, while aflibercept associated very rapidly.

**Evaluation of Ranibizumab and Aflibercept Binding to VEGF Using Sedimentation Velocity Analytical Ultracentrifugation (SV-AUC).** Each molecule and preformed ranibizumab/VEGF and aflibercept/VEGF complex was first evaluated individually to obtain its sedimentation coefficient. The analytical ultracentrifugation data was fitted by the direct boundary model,  $c(s)$ , maximizing the resolution and sensitivity.<sup>15,19,20</sup> The sedimentation coefficients of VEGF, ranibizumab, and aflibercept in PBS, corrected for the standard conditions of water at 20 °C ( $s_{20,w}$ ), were 3.0, 3.7, and 5.2 S, respectively (Figure 3A). The sedimentation coefficients of the 2:1 ranibizumab/VEGF complex and 1:1 aflibercept/VEGF complex were 6.0 and 6.5 S, respectively (Figure 3A).

A competition assay in which a preformed 1:1 complex of aflibercept/VEGF was challenged with 1 mol equiv of free ranibizumab (Figure 3B, dotted line) showed a major peak at 6.2 S, a peak at 3.6 S, and a raised baseline between 4 and 6 S. The peak at 3.6 S is consistent with free ranibizumab (Figure 3A). The main peak at 6.2 S likely represents a mixture of 2:1 complex of ranibizumab/VEGF (6.0 S) and 1:1 complex of aflibercept/VEGF (6.5 S). The raised baseline indicates that the mixture is complex and may also contain free aflibercept. Interestingly, the addition of 2 mol equiv of free ranibizumab to a 1:1 aflibercept/VEGF complex showed a more symmetrical peak at 6.2 S with a distinct shoulder at 5.3 S and a peak at 3.6 S (Figure 3B, solid line). The shoulder at 5.3 S is consistent with free aflibercept and that at 3.6 S with free ranibizumab (Figure 3A), indicating that ranibizumab was able to displace aflibercept from the preformed aflibercept/VEGF complex.

To verify that the peak at 6.2 S contains significant levels of ranibizumab/VEGF complex, ranibizumab was labeled with the Alexa Fluor 488 dye (ranibizumab\*) and the competition experiment was performed with detection using fluorescence optics (Figure 3C). The sedimentation coefficient ( $s_{20,w} = 3.7$  S) for ranibizumab\* alone (inset, Figure 3C) confirmed that the labeling procedure did not change the sedimentation characteristics of ranibizumab. Additionally, the potency was also unaffected (data not shown). The addition of 2 mol equiv of ranibizumab\* to the preformed 1:1 aflibercept/VEGF complex clearly showed a ranibizumab\*/VEGF complex peak at 6.1 S in addition to the free ranibizumab\* peak at 3.7 S. Note that with fluorescence optics, only the fluorescently labeled species (i.e., ranibizumab\* and ranibizumab\* complex) are visible, and any free aflibercept or aflibercept associated complex will not be detected.

The reverse competition experiment was performed where a preformed 2:1 ranibizumab/VEGF complex was challenged with 0.5, 1, and 4 mol equiv of free aflibercept (Figure 3D). In this case, no labeling was used and the detection was achieved with UV optics. The minor peak at 3.4 S is likely a small amount of free ranibizumab. The free ranibizumab peak at 3.4 S remained constant with increasing amount of free aflibercept added to the preformed complex, indicating no large displacement of ranibizumab by aflibercept, even at a 4-fold molar excess of aflibercept. The slight difference observed in the sedimentation coefficient of free ranibizumab (3.4 vs 3.7 S from Figure 3A) is likely due to the known limits of  $c(s)$  analysis to accurately resolve minor peaks.<sup>21</sup> With increasing molar concentrations of free aflibercept, the major peak shifted to a smaller sedimentation coefficient, that is, from 5.8 to 5.7 to 5.6 S at 0.5, 1, and 4 mol equiv of free aflibercept, respectively,

indicating that the peak may consist of a mixture of 2:1 ranibizumab/VEGF complex and increasing levels of free aflibercept that are not well resolved. The following mass balance equations predict this behavior:

$$s_{20,w}(\text{obs}) = [F_{(A)}s_{20,w(A)}] + [F_{(RV)}s_{20,w(RV)}] \quad (1)$$

$$F_{(A)} + F_{(RV)} = 1 \quad (2)$$

$$F_{(A)} = C_{(A)}/C_{\text{total}} \quad (3)$$

where  $F$  is the weight fraction,  $C$  is the concentration in mg/mL, and the subscripts (A) and (RV) indicate free aflibercept and ranibizumab/VEGF complex, respectively.

Equation 1 assumes that the observed sedimentation coefficient is composed of the weight fraction of free aflibercept and ranibizumab/VEGF complex cosedimenting. Equation 2 represents the assumption that free aflibercept and ranibizumab/VEGF complex account for all sedimenting species. Equation 3 defines the weight fraction of free aflibercept as the concentration of aflibercept added to the total protein concentration present.

With  $C_{\text{total}} = 0.1$  mg/mL and the added concentration of aflibercept,  $F_{(A)}$  and  $F_{(RV)}$  can be calculated from eqs 2 and 3. With the measured sedimentation coefficients from Figure 3A,  $s_{20,w(A)} = 5.2$  and  $s_{20,w(RV)} = 6.0$ , the observed sedimentation coefficient [ $s_{20,w}(\text{obs})$ ] can be calculated from eq 1 and compared with the experimentally determined sedimentation coefficients (Table 1).

**Table 1**

$C_{(A)}$	$s_{20,w}$ (calc)	$s_{20,w}$ (obs)
0.030	5.76	5.8
0.046	5.63	5.7
0.770	5.38	5.5

The calculated  $s_{20,w}$  values are in remarkably good agreement with the experimentally observed  $s_{20,w}$  corroborating the notion that the observed shift in the  $s$ -value of the major peak in Figure 3D is likely a consequence of the main peak consisting of unresolved 2:1 ranibizumab/VEGF complex and free aflibercept and that increasing amounts of free aflibercept added to the preformed ranibizumab/VEGF complex does not significantly disrupt this complex.

**Effects of Ranibizumab, Aflibercept, and Bevacizumab on BREC Proliferation.** The inhibitors were compared for their ability to inhibit VEGF-stimulated proliferation of BREC, which is a well-established physiologically relevant cell type to investigate angiogenesis, as detailed in the Materials and Methods section. In three independent experiments (Figure 4 A–C), ranibizumab, aflibercept, and bevacizumab showed dose-dependent inhibition of BREC proliferation induced by 6 ng/mL (0.15 nM) VEGF with average  $IC_{50}$  values of  $0.088 \pm 0.032$ ,  $0.090 \pm 0.009$ , and  $0.500 \pm 0.091$  nM, respectively. Ranibizumab and aflibercept showed very similar potencies, with no statistically significant differences between the two inhibitors ( $P = 0.99$ ). Bevacizumab was approximately 6-fold less potent than ranibizumab and aflibercept ( $P < 0.05$ ; Figure 4D). In agreement with previous potency studies,<sup>12</sup> ranibizumab and aflibercept were equipotent, because in both cases near complete inhibition of BREC proliferation was achieved at the concentration of approximately 0.37 nM. We also performed proliferation assays using 3 ng/mL (0.075 nM)

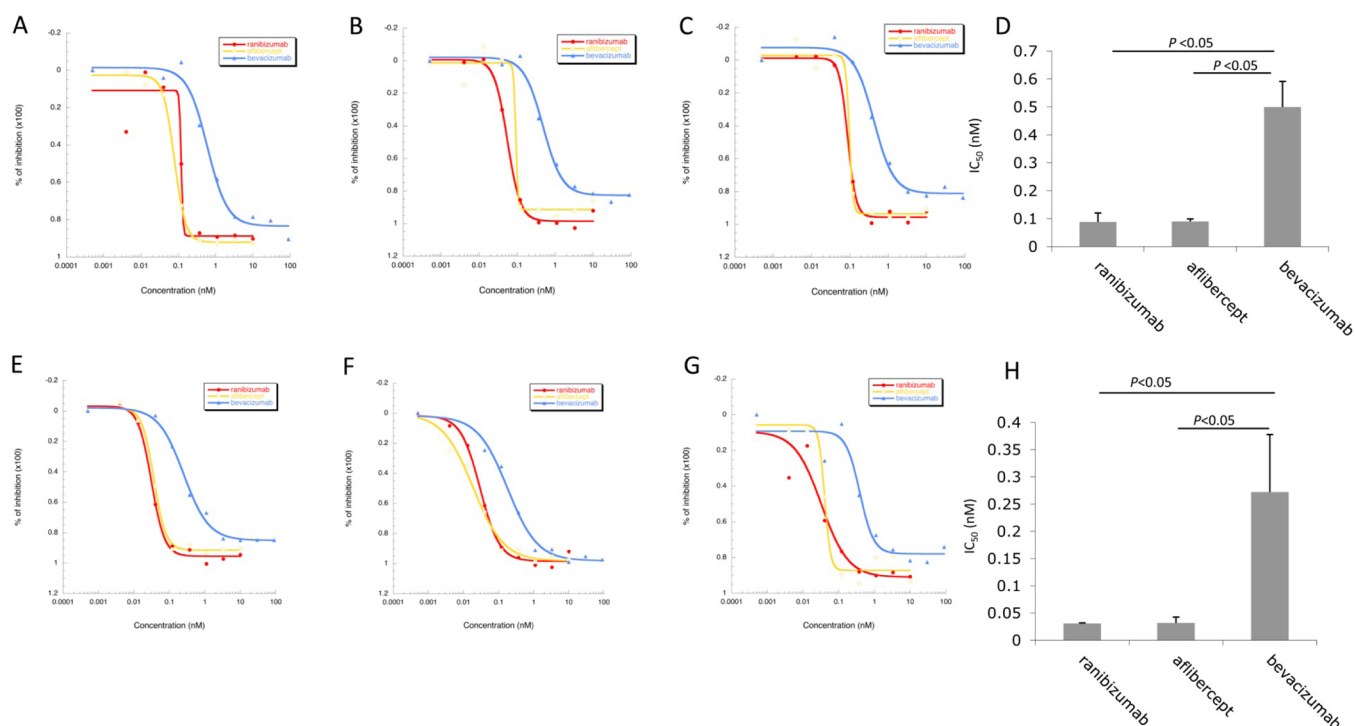


**Figure 4.** Inhibition of VEGF-induced BREc proliferation in the presence of 6 ng/mL (A–C) and 3 ng/mL VEGF (E–G). (D, H) Mean  $IC_{50}$  values; error bars = SD;  $P < 0.05$  versus bevacizumab.

VEGF, to rule out the possibility that the observed lack of difference between ranibizumab and aflibercept might be related to the higher concentration of VEGF. This is nearly the lowest level of VEGF capable of inducing a clearly measurable proliferative response. In multiple experiments in the presence of 3 ng/mL (0.075 nM) VEGF (Figure 4E–G), ranibizumab and aflibercept were found to be equipotent, with average  $IC_{50}$  values of  $0.031 \pm 0.001$  and  $0.032 \pm 0.010$  nM, respectively (Figure 4H). Bevacizumab had an  $IC_{50}$  value of  $0.272 \pm 0.105$  nM, and therefore it was approximately 9-fold less potent than ranibizumab and aflibercept.

## DISCUSSION

Following over two decades of studies and development, Biacore has become one of the most applied technologies in assessing bimolecular interactions, including antibody–antigen binding.<sup>22</sup> Despite many of the advances in the technology, challenges are still encountered in obtaining intrinsic binding affinities and kinetics, especially for biotherapeutics binding to their targets. This is because of the high affinities that sometimes exceed instrument detection limit, the multimeric nature of antibodies and sometimes antigens as well, and the potentially heterogeneous mixture of molecular entities due to post-translational modifications.<sup>18,23</sup> In the present study, when we consider all Biacore data, it is evident that binding affinities and kinetics of all three inhibitors of homodimeric rhVEGF are highly assay format dependent. Specifically, over three assay formats,  $K_D$  values of ranibizumab range from <9.2 to 67 pM, those for bevacizumab from 75.4 to 4456 pM, and those for aflibercept  $K_D$  ( $K_{D1}$ ) from 1.8 to 9263 pM. Interestingly, when VEGF inhibitors are immobilized directly on chips (format 2), the (first) association rate constant values, ( $k_{a1}$ )  $k_a$ , dramatically increase compared with those derived when these inhibitors were in solution (format 1). This might be due to differential

accessibility of the rhVEGF/anti-VEGF molecules when different formats are used. We have observed similar assay format dependencies in other antibody–antigen binding interactions (data not shown), and a similar effect of ligand orientation on binding affinity has been reported.<sup>6</sup> Furthermore, while ranibizumab and bevacizumab showed similar kinetics and affinities in the direct and indirect immobilization formats (formats 2 and 3), aflibercept binding to rhVEGF was dramatically different. In format 3, both the  $k_a$  and  $k_d$  for aflibercept were significantly different from the  $k_{a1}$  and  $k_{d1}$  values derived from format 2, which resulted in the  $K_D$  value derived from format 3 decreasing by over 2000-fold. The reason for this is not clear and needs further investigation, but is not solely due to the different models used. One hypothesis is that the molecular structure of aflibercept (a huIgG1 Fc region fused with two identical VEGF binding sites, each consisting of domains of human VEGFR1 and R2<sup>11</sup>) might have a different flexibility than a conventional antibody or antibody fragment such as bevacizumab (huIgG1) or ranibizumab (Fab). As a result the overall molecular conformation/orientation of aflibercept on a sensor chip might be quite dependent on how the molecule is immobilized and thus result in very different VEGF binding kinetics and affinities using various assay formats.

It is also noted that each assay format has its advantages and caveats. While direct immobilization is often used due to its convenience, a nonspecifically immobilized protein on a sensor chip may have potentially altered binding properties. An indirectly captured protein has the advantage of being oriented in a uniform manner, but it might experience steric hindrance in its binding to target or a potentially altered binding property via allosteric interactions between the capturing reagent and the protein. Format 1 is likely to offer the best Biacore method for direct comparison of binding of the three VEGF inhibitors to rhVEGF where the target is immobilized on a sensor chip, with



the caveat that any potentially altered binding property may not be equally experienced by its inhibitors. So far, no direct evidence is available showing which Biacore-based assay format is most representative of the *in vivo* binding conditions. The assay format dependency together with Biacore detection limit means that Biacore is not the ideal platform for determining the true binding affinities of the three inhibitors for rhVEGF. However, despite this assay format dependency, ranibizumab appeared to be a very tight VEGF binder in all three formats. The results are also very comparable to those reported previously. It should be noted that the indirect capturing method, as used by Papadopoulos et al.,<sup>4</sup> has a fundamental limitation for ranibizumab affinity determination because of significant rapid dissociation of captured ranibizumab from the anti-Fab antibody.

Because of the biological nature of VEGF, a secreted protein, interactions between VEGF and its inhibitors *in vivo* are expected to be best evaluated via solution-based analysis with no modification on either molecule.

The AUC data presented in this study show that both ranibizumab and aflibercept can bind VEGF in solution, as expected (Figure 3A). The competition binding experiments show that ranibizumab is able to displace aflibercept from a preformed aflibercept/VEGF complex (Figure 3B,C). Conversely, excess aflibercept was unable to significantly displace ranibizumab from a preformed ranibizumab/VEGF complex (Figure 3D).

The competition experiments by SV-AUC show the distribution of species present after several hours of co-incubation. While it has not been established that the system is at thermodynamic equilibrium, the interpretation of these results is not dependent on this condition. It is evident that sufficient time for ranibizumab to significantly displace aflibercept from a preformed complex with VEGF was achieved. The results in Figure 3B strongly suggest that ranibizumab is completely displacing aflibercept from VEGF; however, since the detection in this panel is using the absorbance optics, complexes present in solution cannot be cleanly resolved and uniquely identified. Using the fluorescence optics with Alexa Fluor 488 labeled ranibizumab (ranibizumab\*) (Figure 3C) allows unique identification of species in solution where ranibizumab\* is present. The only observable species are free ranibizumab\* and the 2:1 ranibizumab\*/VEGF complex, indicating complete dissociation of the aflibercept/VEGF complex on the time scale of hours. These results are incompatible with previously published affinity data<sup>4</sup> in which aflibercept was proposed to have a ~100-fold lower  $K_D$  for VEGF versus ranibizumab. In these experiments, aflibercept would have both a kinetic and affinity advantage that ranibizumab would not be expected to overcome; however the data in Figure 3 clearly demonstrate that even in the presence of aflibercept, the ranibizumab/VEGF complex is the preferred complex. The reverse experiment, allowing ranibizumab/VEGF to form a complex before the addition of free aflibercept (Figure 3D), shows that aflibercept is unable to displace ranibizumab from VEGF, even when present in a large molar excess. The main peak, observed again using absorbance optics, shifts to lower sedimentation coefficient with increasing aflibercept concentration. The sedimentation coefficient moves toward that of free aflibercept, indicating that the signal is dominated by the free aflibercept and not by aflibercept/VEGF complex in which case the peak should have shifted to a higher  $s$  value.

The displacement of aflibercept from VEGF requires that a ternary complex ranibizumab/VEGF/aflibercept be formed; however, this ternary complex is not observed in the SV-AUC experiments. While the monovalent (i.e., one-armed) affinity of aflibercept for VEGF is not known, it is assumed to be sufficiently weak that the ternary complex is unable to accumulate to detectable levels. Incubating the system to chemical equilibrium would not be expected to allow accumulation of this species since the concentration of all components are well above their reported affinities such that the binding reactions would be expected to go to completion and only the most stable species would be observed.

Since ranibizumab and aflibercept have been developed for intraocular use, BRECs are one of the most relevant cell types that could be used to assay the potency of these VEGF inhibitors. The results indicate that under uniform conditions at two different concentrations of VEGF, ranibizumab, and aflibercept are equipotent with respect to their ability to inhibit the VEGF-induced BREC proliferation, and both had significantly greater potency than bevacizumab. Moreover, it has previously been shown that ranibizumab and aflibercept have similar potency when determined using a HUVEC migration assay.<sup>12</sup>

During drug development, *in vitro* assays of various kinds are used to select candidate molecules for further evaluation and development. It is generally assumed that higher target binding affinity and better cell-based potency will translate into better clinical outcomes. There is seldom an opportunity to evaluate this assumed translatability of *in vitro* assessments of a therapeutic protein to its clinical efficacy. This is primarily because it is uncommon for the same molecule to be targeted by multiple drugs that display such disparate *in vitro* characteristics and have also been compared side-by-side clinically. Herein we have such an opportunity. We have reported here differences in molecular properties and potency between three approved anti-VEGF therapeutics and contrasted them to prior evaluations. Data from large randomized clinical studies have shown that ranibizumab and aflibercept have similar visual acuity outcomes in wet age-related macular degeneration (wAMD).<sup>24,25</sup> In addition, in year two of the VIEW studies when the same as-needed treatment regimen was employed, the durability between ranibizumab and aflibercept was similar. In the CATT and IVAN trials, visual acuity gains were numerically higher for ranibizumab compared with bevacizumab; however, these differences were not statistically significant.<sup>26,27</sup> However, in terms of anatomic outcomes, ranibizumab was statistically significantly better than bevacizumab in resolving macular edema.<sup>27,28</sup> A recent study showed that ranibizumab, a Fab therapeutic with lower systemic exposure relative to bevacizumab,<sup>29</sup> had significantly lower rates of systemic serious adverse events compared with bevacizumab in CATT.<sup>27,28</sup> Importantly, both bevacizumab and aflibercept suppress systemic free-VEGF to a greater extent than ranibizumab,<sup>26,29</sup> raising concerns regarding a potential relationship between the suppression of VEGF and systemic adverse events.<sup>25,30</sup> These data suggest that the translation of *in vitro* data to clinical efficacy is not linear and that *in vitro* assessments of affinity or potency are unlikely to be useful in predicting clinical differences between drugs, particularly when dealing with high affinity molecules. This idea is further supported by some recent modeling data showing that improvements in  $K_D$  and intravitreal half-life have little effect on visual acuity outcomes for anti-VEGF therapeutics.<sup>31</sup>

## CONCLUSION

In conclusion, we demonstrate that binding affinity measurements for VEGF inhibitors using SPR are assay format dependent, and therefore caution must be exercised in designing experiments and interpreting results. Moreover, data from the AUC experiments, a direct solution phase method for assessing molecular interactions, and BREC proliferation assays do not support claims that aflibercept binds and inhibits VEGF with higher affinity and potency than ranibizumab. While optimizing therapeutic candidates to enhance their binding affinities is often useful in developing efficacious drugs, the contribution of affinity alone should always be interpreted in the context of mechanism of action of the drug and disease biology.<sup>32</sup> In fact, it has been reported that a lower affinity anti-TfR variant showed improved brain uptake of the molecule compared with a high affinity variant, resulting in successful development of a therapeutic candidate for treating Alzheimer's disease.<sup>33</sup> Taking all into consideration, including results of the BREC assay, as well as recent clinical trial results in AMD,<sup>24,34</sup> it appears that the affinities of ranibizumab and aflibercept binding to their target, VEGF, are sufficient to result in similar clinical potency and durability.

## AUTHOR INFORMATION

### Corresponding Author

\*Sandeep Yadav, Ph.D. E-mail: Yadav.sandeep@gene.com. Phone: (650) 225 8912. Fax: (650) 742 1504.

### Present Address

†(N.F.) University of California, San Diego, La Jolla, California 92093, United States

### Notes

The authors declare no competing financial interest.

## ACKNOWLEDGMENTS

This study was sponsored by Genentech, Inc., South San Francisco, California. Genentech, Inc. is a member of the Roche Group. The authors are employees of Genentech, Inc. Support for third-party writing assistance for this manuscript was provided by Genentech, Inc.

## NONSTANDARD ABBREVIATIONS

AMD, age-related macular degeneration; AUC, analytical ultracentrifugation; BREC, bovine retinal microvascular endothelial cell; DME, diabetic macular edema;  $k_a$ , association rate constant;  $K_D$ , dissociation equilibrium constant;  $k_d$ , dissociation rate constant; rhVEGF, recombinant human vascular endothelial growth factor; RU, resonance unit; RVO, retinal vein occlusion; SPR, surface plasmon resonance; SV-AUC, sedimentation velocity analytical ultracentrifugation; VEGF, vascular endothelial growth factor A

## REFERENCES

- (1) Ferrara, N.; Damico, L.; Shams, N.; Lowman, H.; Kim, R. Development of ranibizumab, an anti-vascular endothelial growth factor antigen binding fragment, as therapy for neovascular age-related macular degeneration. *Retina* **2006**, *26* (8), 859–870.
- (2) Lowe, J.; Araujo, J.; Yang, J.; Reich, M.; Oldendorf, A.; Shiu, V.; Quarmby, V.; Lowman, H.; Lien, S.; Gaudreault, J.; Maia, M. Ranibizumab inhibits multiple forms of biologically active vascular endothelial growth factor in vitro and in vivo. *Exp. Eye Res.* **2007**, *85* (4), 425–430.
- (3) Presta, L. G.; Chen, H.; O'Connor, S. J.; Chisholm, V.; Meng, Y. G.; Krummen, L.; Winkler, M.; Ferrara, N. Humanization of an anti-

vascular endothelial growth factor monoclonal antibody for the therapy of solid tumors and other disorders. *Cancer Res.* **1997**, *57* (20), 4593–4599.

- (4) Papadopoulos, N.; Martin, J.; Ruan, Q.; Rafique, A.; Rosconi, M. P.; Shi, E.; Pyles, E. A.; Yancopoulos, G. D.; Stahl, N.; Wiegand, S. J. Binding and neutralization of vascular endothelial growth factor (VEGF) and related ligands by VEGF Trap, ranibizumab and bevacizumab. *Angiogenesis* **2012**, *15* (2), 171–185.

- (5) *Handbook of Surface Plasmon Resonance*; RSC Publishing: Enschede, the Netherlands, 2007.

- (6) Trilling, A. K.; Harmsen, M. M.; Ruigrok, V. J. B.; Zuilhof, H.; Beekwilder, J. The effect of uniform capture molecule orientation on biosensor sensitivity: Dependence on analyte properties. *Biosens. Bioelectron.* **2013**, *40* (1), 219–226.

- (7) O'Shannessy, D. J. Determination of kinetic rate and equilibrium binding constants for macromolecular interactions: A critique of the surface plasmon resonance literature. *Curr. Opin. Biotechnol.* **1994**, *5* (1), 65–71.

- (8) Yadav, S.; Liu, J.; Scherer, T. M.; Gokarn, Y.; Demeule, B.; Kanai, S.; Andya, J. D.; Shire, S. J. Assessment and significance of protein-protein interactions during development of protein biopharmaceuticals. *Biophys. Rev.* **2013**, *5*, 121–136.

- (9) Kroe, R. R.; Laue, T. M. NUTS and BOLTS: Applications of fluorescence-detected sedimentation. *Anal. Biochem.* **2009**, *390* (1), 1–13.

- (10) MacGregor, I. K.; Anderson, A. L.; Laue, T. M. Fluorescence detection for the XLI analytical ultracentrifuge. *Biophys. Chem.* **2004**, *108* (1–3), 165–185.

- (11) Holash, J.; Davis, S.; Papadopoulos, N.; Croll, S. D.; Ho, L.; Russell, M.; Boland, P.; Leidich, R.; Hylton, D.; Burova, E.; Ioffe, E.; Huang, T.; Radziejewski, C.; Bailey, K.; Fandl, J. P.; Daly, T.; Wiegand, S. J.; Yancopoulos, G. D.; Rudge, J. S. VEGF-Trap: A VEGF blocker with potent antitumor effects. *Proc. Natl. Acad. Sci. U. S. A.* **2002**, *99* (17), 11393–11398.

- (12) Yu, L.; Liang, X. H.; Ferrara, N. Comparing protein VEGF inhibitors: In vitro biological studies. *Biochem. Biophys. Res. Commun.* **2011**, *408* (2), 276–281.

- (13) LUCENTIS (ranibizumab injection). Highlights of Prescribing Information. Available at [http://www.gene.com/download/pdf/lucentis\\_prescribing.pdf](http://www.gene.com/download/pdf/lucentis_prescribing.pdf).

- (14) EYLEA (aflibercept injection). Highlights of Prescribing Information. Available at <http://www.regeneron.com/Eylea/eylea-fpi.pdf>.

- (15) Schuck, P. Size-distribution analysis of macromolecules by sedimentation velocity ultracentrifugation and lamm equation modeling. *Biophys. J.* **2000**, *78* (3), 1606–1619.

- (16) Leung, D. W.; Cachianes, G.; Kuang, W. J.; Goeddel, D. V.; Ferrara, N. Vascular endothelial growth factor is a secreted angiogenic mitogen. *Science* **1989**, *246* (4935), 1306–1309.

- (17) Karlsson, R.; Falt, A. Experimental design for kinetic analysis of protein-protein interactions with surface plasmon resonance biosensors. *J. Immunol. Methods* **1997**, *200* (1–2), 121–133.

- (18) Muller, K. M.; Arndt, K. M.; Pluckthun, A. Model and simulation of multivalent binding to fixed ligands. *Anal. Biochem.* **1998**, *261* (2), 149–158.

- (19) Schuck, P.; Perugini, M. A.; Gonzales, N. R.; Howlett, G. J.; Schubert, D. Size-distribution analysis of proteins by analytical ultracentrifugation: Strategies and application to model systems. *Biophys. J.* **2002**, *82* (2), 1096–1111.

- (20) Schuck, P. On computational approaches for size-and-shape distributions from sedimentation velocity analytical ultracentrifugation. *Eur. Biophys. J.* **2010**, *39* (8), 1261–1275.

- (21) Gabrielson, J. P.; Arthur, K. K.; Stoner, M. R.; Winn, B. C.; Kendrick, B. S.; Razinkov, V.; Svitel, J.; Jiang, Y.; Voelker, P. J.; Fernandes, C. A.; Ridgeway, R. Precision of protein aggregation measurements by sedimentation velocity analytical ultracentrifugation in biopharmaceutical applications. *Anal. Biochem.* **2010**, *396* (2), 231–241.

(22) Cannon, M. J.; Myska, D. G. Surface Plasmon Resonance. In *Methods for Structural Analysis of Protein Pharmaceuticals*; Jiskoot, W., Crommelin, D., Eds.; AAPS Press: Arlington, VA, 2005; Vol. 3, pp 527–544.

(23) Drake, A. W.; Myska, D. G.; Klakamp, S. L. Characterizing high-affinity antigen/antibody complexes by kinetic- and equilibrium-based methods. *Anal. Biochem.* **2004**, *328* (1), 35–43.

(24) Heier, J. S.; Brown, D. M.; Chong, V.; Korobelnik, J. F.; Kaiser, P. K.; Nguyen, Q. D.; Kirchhof, B.; Ho, A.; Ogura, Y.; Yancopoulos, G. D.; Stahl, N.; Vitti, R.; Berliner, A. J.; Soo, Y.; Anderesi, M.; Groetzbach, G.; Sommerauer, B.; Sandbrink, R.; Simader, C.; Schmidt-Erfurth, U.; VIEW 1 and VIEW 2 Study Groups. Intravitreal aflibercept (VEGF Trap-Eye) in wet age-related macular degeneration. *Ophthalmology* **2012**, *119* (12), 2537–2548.

(25) Schmidt-Erfurth, U.; Kaiser, P. K.; Korobelnik, J. F.; Brown, D. M.; Chong, V.; Nguyen, Q. D.; Ho, A. C.; Ogura, Y.; Simader, C.; Jaffe, G. J.; Slakter, J. S.; Yancopoulos, G. D.; Stahl, N.; Vitti, R.; Berliner, A. J.; Soo, Y.; Anderesi, M.; Sowade, O.; Zeitz, O.; Norenberg, C.; Sandbrink, R.; Heier, J. S. Intravitreal aflibercept injection for neovascular age-related macular degeneration: Ninety-six-week results of the VIEW studies. *Ophthalmology* **2014**, *121* (1), 193–201.

(26) Chakravarthy, U.; Harding, S. P.; Rogers, C. A.; Downes, S. M.; Lotery, A. J.; Wordsworth, S.; Reeves, B. C.; IVAN Study Investigators. Ranibizumab versus bevacizumab to treat neovascular age-related macular degeneration: One-year findings from the IVAN randomized trial. *Ophthalmology* **2012**, *119* (7), 1399–1411.

(27) Martin, D. F.; Maguire, M. G.; Ying, G. S.; Grunwald, J. E.; Fine, S. L.; Jaffe, G. J.; CATT Research Group. Ranibizumab and bevacizumab for neovascular age-related macular degeneration. *N. Engl. J. Med.* **2011**, *364* (20), 1897–1908.

(28) Martin, D. F.; Maguire, M. G.; Fine, S. L.; Ying, G. S.; Jaffe, G. J.; Grunwald, J. E.; Toth, C.; Redford, M.; Ferris, F. L., 3rd. Comparison of Age-related Macular Degeneration Treatments Trials (CATT) Research Group. Ranibizumab and bevacizumab for treatment of neovascular age-related macular degeneration: Two-year results. *Ophthalmology* **2012**, *119* (7), 1388–1398.

(29) Avery, R. L.; Castellarin, A. A.; Steinle, N. C.; Dhoot, S. D.; Pieramici, D. J.; See, R.; Couvillion, S.; Nasir, M. A.; Rabena, M. D.; Le, K.; Maia, M.; Visich, J. E. Systemic pharmacokinetics following intravitreal injections of ranibizumab, bevacizumab or aflibercept in patients with neovascular AMD. *Br. J. Ophthalmol.* **2014**, DOI: 10.1136/bjophthalmol-2014-305252.

(30) Avery, R. What is the evidence for systemic effects of intravitreal anti-VEGF agents, and should we be concerned? *Br. J. Ophthalmol.* **2014**, *98* (Suppl 1), i7–i10.

(31) Le, K.; Lu, T.; Visich, J. A semi-mechanistic PKPD model describing visual acuity as a function of the affinity and intravitreal half-life of intraocular anti-VEGF agents in age-related macular degeneration. Presented at the American Society for Clinical Pharmacology and Therapeutics Annual Meeting, Indianapolis, IN, 2013.

(32) Copeland, R. A.; Pompliano, D. L.; Meek, T. D. Drug-target residence time and its implications for lead optimization. *Nat. Rev. Drug Discovery* **2007**, *6* (3), 249–249.

(33) Yu, Y. J.; Zhang, Y.; Kenrick, M.; Hoyte, K.; Luk, W.; Lu, Y. M.; Atwal, J.; Elliott, J. M.; Prabhu, S.; Watts, R. J.; Dennis, M. S. Boosting brain uptake of a therapeutic antibody by reducing its affinity for a transcytosis target. *Sci. Transl. Med.* **2011**, *3* (84), 1–8.

(34) Heier, J. S.; Brown, D. M.; Chong, V.; Korobelnik, J. F.; Kaiser, P. K.; Nguyen, Q. D.; Kirchhof, B.; Ho, A.; Ogura, Y.; Yancopoulos, G. D.; Stahl, N.; Vitti, R.; Berliner, A. J.; Soo, Y.; Anderesi, M.; Groetzbach, G.; Sommerauer, B.; Sandbrink, R.; Simader, C.; Schmidt-Erfurth, U.; VIEW 1 and VIEW 2 Study Groups. Erratum: Intravitreal aflibercept (VEGF Trap-Eye) in wet age-related macular degeneration. *Ophthalmology* **2013**, *120* (1), 209–210.